Quantum Machine Intelligence (2026) 8:11
https://doi.org/10.1007/s42484-026-00343-2

RESEARCH ARTICLE

Positive-unlabeled learning for training an entanglement detector

Taisei Nohara[1] · **Itsuki Noda**[2] · **Satoshi Oyama**[3]

Received: 30 May 2025 / Accepted: 7 January 2026

Abstract
Entanglement detection, the process of verifying quantum entanglement is a fundamental challenge in quantum information processing. Various approaches have been proposed to address this challenge, with many recent studies applying supervised machine learning methods. While these methods have demonstrated high accuracy in entanglement detection, it is reasonable to assume that the entangled states themselves are not definitively known. To address this limitation, we have devised a machine learning method for entanglement detection based on positive-unlabeled learning, a classical machine learning framework that does not use label information from negative data. Using a deep neural network model to synthetic dataset under the assumption of mixed states, we conducted experiments on a classical computer to valid the effectiveness and characteristics of the proposed method. Our approach introduces a novel framework that accounts for the data generation constraints in the training process of entanglement detector, thereby advancing machine learning techniques in quantum information science.

Keywords Entanglement detection · Positive-unlabeled learning · Binary classification · Machine learning

1 Introduction

Quantum entanglement plays a central role in quantum information processing. For example, quantum teleportation (Horodecki et al. 1999), quantum computation (Shor 1994; Grover 1996), and quantum cryptography (Bennett and Brassard 2014) utilize quantum entanglement to perform calculations not possible with classical computers. Furthermore, quantum entanglement is an indispensable element in frameworks that rely on quantum states. Quantum states are typically governed by quantum circuits, and verifying entanglement generation at runtime is essential to ensure that the algorithms and subroutines executed by these circuits function properly. Entanglement detection refers to the problem of determining whether a given quantum state is entangled, a problem that has been studied for an extended period (Gühne and Tóth 2009).

In the case of a general bipartite quantum system, entanglement detection is known to be NP-hard (Gurvits 2003). Consequently, numerous studies on entanglement detection have been conducted to achieve higher accuracy. The Peres–Horodecki criterion (Peres 1996; Horodecki et al. 1996), also known as PPT (positive partial transpose) criterion, is one of the most well-known criteria for determining whether a quantum state is entangled. This criterion serves as a powerful tool for analytically determining entangled states from the density matrix within a specific system. However, applying such analytical approaches to relatively large systems is challenging, and no universally applicable method has been established.

As a result, numerous studies in recent years have explored classical machine learning techniques as alternative approaches to entanglement detection (Sanavio et al. 2023; Greenwood et al. 2023). In various machine learning methods, quantum states are categorized as either separable or entangled, framing the problem as a binary classification

✉ Satoshi Oyama
oyama@ds.nagoya-cu.ac.jp

Taisei Nohara
arahon243@eis.hokudai.ac.jp

Itsuki Noda
i.noda@ist.hokudai.ac.jp

[1] Graduate School of Information Science and Technology, Hokkaido University, Sapporo, Hokkaido, Japan

[2] Faculty of Information Science and Technology, Hokkaido University, Sapporo, Hokkaido, Japan

[3] Graduate School of Data Science, Nagoya City University, Nagoya, Aichi, Japan

Published online: 05 February 2026

task. This framing offers the advantage of being both intuitive and readily applicable. In fact, such methods have demonstrated highly accurate entanglement detection.

Although the use of binary classification is reasonable, there is fundamental issue regarding the assumption of training data. An ordinary binary classification problem in machine learning operates on the basis of the availability of both positive and negative example data. However, in the entanglement detection problem, explicitly preparing data representing entangled states is generally challenging. That means it is not possible to guarantee that a quantum state is entangled solely on the basis of the given density matrix. Specific types of entangled states, such as the GHZ state and the W state, can be prepared; however, identifying a quantum state as entangled requires information about the data generation process. This raises the question of how to generate a dataset for training.

Chen et al. (2021) identified challenges in the generation of entangled state data and presented a learning method that does not require explicit entangled state data in the training dataset. They proposed using an unsupervised learning setting in which only data of separable states are assumed to be available. That means no label information is provided in the training dataset. A generative adversarial network (GAN) model along with Siamese neural network is used to train the discriminator and generator using only data from separable states. We believe that avoiding the use of explicit entanglement state data is an effective approach to address the challenge of preparing it, as they demonstrated.

We present a method for addressing the entanglement detection problem in a multi-qubit system that utilizes separable and randomly generated quantum state data while accounting for data availability. The idea of utilizing random quantum states is based on learning from positive-unlabeled data, which is often referred to as PU learning, a classical machine learning framework that does not use label information from negative data (Elkan and Noto 2008). In the PU learning framework, all negative data and a portion of the positive data are provided as unlabeled data, which means that methods for regular supervised learning cannot be directly applied as they assume label information is available for all data. There are several benefits of applying methods based on PU learning: a more realistic setting compared with formulation as regular binary classification and the ability to utilize a broader range of data compared with the setting that includes only separable state data.

Our contributions are as follows:

- We devised a learning method for entanglement detection that does not rely on explicit entangled state data and uses the concept of PU learning. Since reliably generating arbitrary entangled state data in the quantum state generation process is challenging, constructing a training dataset presents difficulties. However, the challenge of generating quantum state data that is definitively either separable or entangled—that is, valid quantum state data—is relatively minor. Our approach prioritizes the availability of quantum state data and offers a method that is more practical for experimental implementation than conventional approaches requiring explicitly entangled state data.
- We developed a method for generating dense datasets that define classification boundaries in fully-separable state detection, enabling the evaluation of a trained model for entanglement detection. Through experimental verification, we demonstrated that the proposed method achieves satisfactory performance on such datasets.
- The effectiveness of the proposed method was verified using a synthetic dataset representing mixed states ranging from 2 to 6 qubits. The proposed PU learning-based method exhibited significantly higher AUC scores compared with two baseline one-class methods, reinforcing the effectiveness of the proposed method.

2 Background

2.1 Problem setting

In this paper we consider a variant of PU learning and aim to obtain accurate inference for new input data, provided as density matrices representing quantum states. For a given integer $n \geq 2$, which determines the dimensions of the input matrix, let $\mathcal{X} \subset \mathbb{C}^{2^n \times 2^n}$ denote the data space and let $\mathcal{Y} = \{+1, -1\}$ denote the output space. We assume that the input data consists of $2^n \times 2^n$ complex matrices in $\mathcal{X}$, with some of the data provided as positive examples of size m_{pos}, denoted by $\mathcal{D}_{pos} = \{\rho_1^{pos}, \ldots, \rho_{m_{pos}}^{pos}\}$, and as unlabeled examples of size m_{unl}, denoted by $\mathcal{D}_{unl} = \{\rho_1^{unl}, \ldots, \rho_{m_{unl}}^{unl}\}$. Defining the decision function and true labeling function to be $f, f^* : \mathcal{X} \to \mathcal{Y}$, which means $f^*(\rho_k^{pos}) = +1$ for $k = 1, \ldots, m_{pos}$, our goal is to identify the f that minimizes the expectation $\mathbb{E}_{\rho \sim P(\rho)}[f(\rho) - f^*(\rho)]$ under data probability distribution $P(\rho)$.

In addition, we assume access to class prior information $\pi_p = Pr(f^*(\rho) = +1)$ and that the data distribution is consistent between the training and test datasets.

2.2 Quantum state and density matrix representation

In quantum mechanics, the state of a physical system is fundamentally described by a complex unit vector in a Hilbert

space $\mathcal{H}$. Such a vector is called a state vector, and the space in which a state vector can take values is referred to as the state space. A state vector is usually denoted by $|\psi\rangle$, while the notation $\langle\psi|$ represents its conjugate transpose.

A fundamental example of quantum system is the one-qubit system, which has two basis states. We denote the concrete state vector as $|\psi\rangle = [\alpha\,\beta]^T = \alpha|0\rangle + \beta|1\rangle$, where $|0\rangle, |1\rangle$ are elements of the computational basis; i.e., $|0\rangle = [1\,0]^T$, $|1\rangle = [0\,1]^T$ and $|\alpha|^2 + |\beta|^2 = 1$. A qubit is considered an extension of the classical bit, which simply takes a value of 0 or 1. Although there are many ways to define the basis, we use the computational basis throughout this paper. More generally, quantum systems can have discrete bases with more than two states, and fundamental discussions regarding qubits can often be extended to such systems in essence.

These expressions can be easily extended to an *n*-qubit system, a system in which a quantum state is represented using 2^n basis states. An *n*-qubit pure state is denoted here as $|\psi\rangle = [\alpha_1, \ldots, \alpha_{2^n}]^T = \sum_{k=1}^{2^n} \alpha_k |k\rangle$, where $|k\rangle$ is a basis vector with its *k*-th element equal to 1 and all other elements equal to 0. The coefficients satisfy the normalization condition $\sum_{k=1}^{2^n} |\alpha_k|^2 = 1$.

A qubit system's behavior can be described through state vector representations, but not all of them. A quantum state that can be expressed by a single vector, such as $|\psi\rangle$, is classified as a pure state. However, there are instances in which a quantum state is represented as a probability weighted mixture of pure states. For example, a quantum state may consist of 40% of $|0\rangle$ and 60% of $|1\rangle$. A density matrix, denoted here by ρ, can be used to describe such a quantum state. Given a set of tuples $(p_k, |\psi_k\rangle)$, where p_k denotes the probability weight of state $|\psi_k\rangle$, the density matrix for the system is defined as $\rho = \sum_k p_k |\psi_k\rangle\langle\psi_k|$. In an *n*-qubit system, the density matrix takes the form of a $2^n \times 2^n$ Hermitian matrix.

Similar to the constraint $\sum_{k=1}^{2^n} |\alpha_k|^2 = 1$ for the *n*-qubit pure state $|\psi\rangle = \sum_{k=1}^{2^n} \alpha_k |k\rangle$, density matrix ρ does not span the entire $2^n \times 2^n$ Hermitian matrix space. The constraints governing ρ are outlined as follows.

Theorem 1 *(Characterization of n-qubit density matrices, Theorem 2.5 in Nielsen and Chuang (2010)[1]) A $2^n \times 2^n$ Hermitian matrix ρ is classified as a density matrix for an n-qubit system if and only if it satisfies the following two conditions:(i) $Tr[\rho] = 1$ and (ii) $\langle\psi|\rho|\psi\rangle \geq 0$ for any n-qubit state vector $|\psi\rangle$.*

[1] Although this theorem is stated in the source text as defining the conditions for the density operator, we reinterpret it in terms of the density matrix, as that is our focus.

Here, we note that this paper does not address the specifics of obtaining the density matrix. Instead, we assume access to its exact values. In experimental settings, estimates—such as expected values—derived from repeated measurements that depend on the elements of the exact density matrix are often used (Thew et al. 2002; Huang et al. 2020).

2.3 Detailed formalization of entanglement detection

Entanglement is a fundamental characteristic of quantum systems, and identifying its presence in an input quantum state is a critical challenge in the field of quantum information. The simplest formulation of the entanglement detection problem occurs in a two-qubit system; which is defined as follows.

Definition 1 (Entanglement detection in a two-qubit system, Definition 3 in Gühne and Tóth (2009)) Given a quantum state represented by a two-qubit density matrix ρ, entanglement detection is the problem of determining whether there exists a set of tuples $(p_k, \rho_k^A, \rho_k^B)_{k=1}^M$ that satisfies $\rho = \sum_{k=1}^M p_k \rho_k^A \otimes \rho_k^B$, subject to the conditions that $p_k \in (0, 1]$ and $\sum_{k=1}^M p_k = 1$ and that ρ_k^A and ρ_k^B are one-qubit density matrices for $k = 1, \ldots, M$. The state ρ is classified as separable if such a set exists and entangled otherwise.

For systems containing more than two qubits, the classification of quantum states becomes increasingly complex due to the presence of multiple types of separability and entanglement. In this paper we primarily focus on distinguishing fully-separable states from other quantum states and define the problem in this case as follows.

Definition 2 (Entanglement detection problem for fully-separability) Given a quantum state represented by a *n*-qubit density matrix ρ, the entanglement detection problem for fully-separability is to determine whether there is a set of tuples $(p_k, \rho_k^1, \rho_k^2, \ldots, \rho_k^n)_{k=1}^M$ that satisfies $\rho = \sum_{k=1}^M p_k \rho_k^1 \otimes \rho_k^2 \otimes \ldots \otimes \rho_k^n$, subject to the conditions that $p_k \in (0, 1]$, that $\sum_{k=1}^M p_k = 1$, and that $\rho_k^1, \rho_k^2, \ldots, \rho_k^n$ are one-qubit density matrices for $k = 1, \ldots, M$. The state ρ is classified as fully-separable if such a set exists; otherwise, it is not fully-separable.

Illustration of the types of entanglement in two-qubit and three-qubit systems are shown in Fig. 1. In a two-qubit system, as defined in Definition 1, each quantum state is

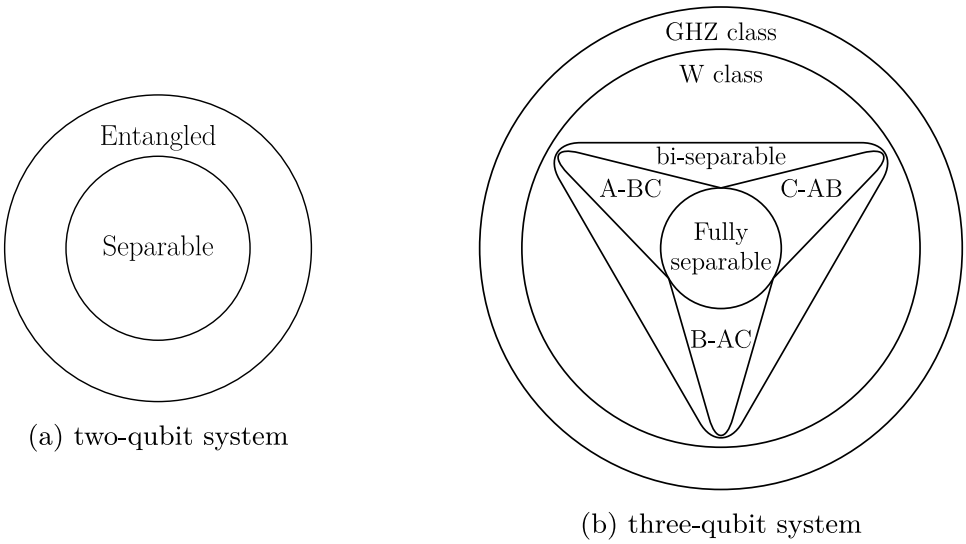

(a) two-qubit system

(b) three-qubit system

Fig. 1 Illustrations of types of entanglement in two-qubit and three-qubit systems. The set of separable states definitively forms a convex set

classified as either separable or entangled. In a three-qubit system, as defined in Dür et al. (2000), the classification of quantum states is more complicated due to the presence of six types of entanglement: fully-separable, bi-separable (A-BC, B-AC, C-AB), and genuine multipartite entanglement (GME) (GHZ class, W class). States exhibiting GME possess the highest degree of entanglement among three-qubit states. Bi-separable states, on the other hand, are those that are neither fully-separable in Definition 2, nor classified as GME states. Strictly speaking, some states in the mixed state set are neither bi-separable nor GME (in three-qubit systems, neither GHZ class nor W class). However, these states are typically regarded as part of the bi-separable set, which ensures convexity and simplifies their mathematical treatment. Similarly, for a general n-qubit system, we can define a set of $k(1 \leq k \leq n)$-separable states, with all of them being regarded as convex (Gabriel et al. 2010).

2.4 Existing approaches for entanglement detection

Entanglement detection has been investigated over the years within the field of quantum information science, and various approaches have been taken. Here, we briefly describe the methods that are most relevant to this study.

PPT criterion The PPT criterion (Peres 1996; Horodecki et al. 1996) is among the earliest established methods for detecting entanglement in small systems and is defined as follows.

Theorem 2 *(PPT criterion (Peres 1996; Horodecki et al. 1996)) Given an n-qubit density matrix ρ, ρ exhibits positive partial transposition if ρ is separable. In particular, when $n = 2$, ρ is separable if ρ is exhibits PPT; that is, these conditions are both necessary and sufficient.*

By using the PPT criterion, we can examine examples that illustrate the boundary between separable and entangled states in two-qubit systems, as explained below.

Example 1 (Bell state under depolarizing noise) Let $\rho(p)$ be a two-qubit density matrix expressed as $\rho(p) = (1-p)\rho_{bell} + p\frac{I}{4}$, where ρ_{bell} represents the Bell state density matrix and I denotes the identity matrix.

$$\rho_{bell} = \frac{1}{2}\begin{pmatrix} 1 & 0 & 0 & 1 \\ 0 & 0 & 0 & 0 \\ 0 & 0 & 0 & 0 \\ 1 & 0 & 0 & 1 \end{pmatrix}, \; I = \begin{pmatrix} 1 & 0 & 0 & 0 \\ 0 & 1 & 0 & 0 \\ 0 & 0 & 1 & 0 \\ 0 & 0 & 0 & 1 \end{pmatrix}.$$

By calculating the partial transpose of $\rho(p)$, we determine that its eigenvalues are $\frac{2-p}{4}$ and $\frac{2-3p}{4}$. Consequently, $\rho(p)$ is separable when $p \in [\frac{2}{3}, 1]$ and entangled when $p \in [0, \frac{2}{3})$.

The PPT criterion is a powerful tool in that it can perfectly identify the separability of a given state; however, it cannot be applied to systems with more than two qubits. In quantum systems comprising three or more qubits, an alternative approach is required to detect entanglement.

Entanglement witness An entanglement witness is an operator that distinguishes a particular entangled state from fully-separable states and is defined as follows.

Definition 3 (Entanglement witness) Given an n-qubit density matrix ρ_{ent} known to be entangled (that is, not fully-separable) and letting S denote the set of density matrices corresponding to fully-separable states on n

qubits, an operator W is called an entanglement witness if $Tr[W\rho_{sep}] \geq 0$ for any $\rho_{sep} \in S$.

Conceptually, entanglement witnesses have no upper limit on the size of the quantum system to which they can be applied, so they can be applied to systems with three or more qubits. In addition, we can found that an unknown input state ρ is entangled if the output satisfies $Tr[W\rho] < 0$. On the other hand, an entanglement witness cannot distinguish entangled states when the range of possible entangled states is extensive.[2] Furthermore, even when an entanglement witness is applicable, determining the appropriate operator W to serve as the witness is generally nontrivial, and research is underway to identify a more suitable witness operator (Zhou et al. 2019).

Entanglement measures There are various indicators for quantifying the strength of entanglement, such as entanglement entropy (Von Neumann entropy) and relative entropy. Among the various entanglement metrics, negativity is particularly relevant to our problem setting. Negativity is defined as follows.

Definition 4 (Negativity, Eq. (1) in Vidal and Werner (2002)) Given a density matrix ρ, negativity for subsystem A is defined as $\mathcal{N}(\rho) = (\|\rho^{T_A}\|_1 - 1)/2$, where ρ^{T_A} denotes the partial transpose of ρ for subsystem A and $\|\cdot\|_1$ denotes the trace norm.

Negativity can be interpreted as a type of penalty within the PPT criterion. Since an input density matrix ρ being PPT and the negativity of ρ being zero are equivalent, in a two-qubit system, a negativity of zero corresponds to ρ being separable. A notable advantage of negativity is that it is a computable measure for mixed state inputs, whereas other measures, such as entanglement entropy, primarily apply to pure states.

2.5 Methods for anomaly detection

Although the primary focus of this paper is on entanglement detection using PU learning, a one-class classification model is used to establish baseline methods for subsequent experiments. We will briefly explain existing methods for one-class classification. Let $\mathcal{X} \subset \mathbb{R}^d$ denote the data space. Given unlabeled data $\{\boldsymbol{x}_1, \ldots, \boldsymbol{x}_m\} \subset \mathcal{X}$, anomaly detection is the problem of determining whether newly received data are normal or anomalous.

[2] Specifically, in cases where the convex hull of the possible entangled states overlaps with the set of fully-separable states, no witness exists that can perfectly distinguish these states by the value of $Tr[W\rho]$, which is a linear function of ρ.

One commonly used method for the anomaly detection problem is the support vector data description (SVDD) method (Tax and Duin 2004). SVDD solves the following optimization problem: $\min_{R,\xi_k,\boldsymbol{a}} R^2 + C\sum_{k=1}^{m}\xi_k$ subject to $\|\boldsymbol{x}_k - \boldsymbol{a}\|_2^2 \leq R^2 + \xi_k$ for $k = 1, \ldots, m$. Intuitively, SVDD searches for the minimal hypersphere that surrounds the given data $\boldsymbol{x}_1, \ldots, \boldsymbol{x}_m$. In this formulation, C is a positive constant that determines the looseness of the solution, and $\{\xi_k\}_{k=1}^m$ is a variable that determines the extent to which ξ_i is allowed to deviate from the center $\boldsymbol{a}$. By using kernel functions in the calculation of the inner product among vectors $\boldsymbol{x}_1, \ldots, \boldsymbol{x}_m, \boldsymbol{a}$, more diverse data boundaries can be explored in different feature spaces.

Deep SVDD (Ruff et al. 2018) is a one-class classification method based on deep learning and the SVDD concept. Analogous to SVDD, Deep SVDD uses a deep neural network model to learn a feature map, enabling more flexible boundary detection. One-Class Deep SVDD was introduced in Ruff et al. (2018) as a variant of Deep SVDD under the assumption that most of the training data are normal. The objective function for One-Class Deep SVDD is defined as

$$\min_W \frac{1}{m}\sum_{k=1}^{m}\|\phi(\boldsymbol{x}_k; W) - \boldsymbol{a}\|_2^2 + \frac{\lambda}{2}\sum_{k=1}^{L}\|W^k\|_F^2,$$

where W^k represents the weights of the network $\phi(\cdot)$ in the k-th layer, and $W = \{W^k\}_{k=1}^L$ represents the set of weights across all layers. The hyperparameter λ serves as the network weight decay regularizer. This objective function was designed under the assumption that most of the training data are normal, leading to the mapping of the data near representation $\boldsymbol{a}$. For details on general methods related to one-class classification, refer to Seliya et al. (2021).

2.6 Learning using unlabeled data

Positive-unlabeled learning is a classical machine learning approach using positive and unlabeled data that addresses the problem of learning from incomplete label information (Elkan and Noto 2008; Zhao et al. 2022; Bekker and Davis 2020). This problem shares core principles with regular binary classification, although it differs in terms of accessibility to label information (see Fig. 2). Two label are used: positive and unlabeled. A positive label indicated that the datum is truly positive, and an unlabeled datum means that there is uncertainty about whether the datum belongs to the positive or negative category. It is essential to use unlabeled data for learning in the PU learning framework. This approach can be applied to other problem settings (Ju et al. 2020; Takahashi et al. 2024).

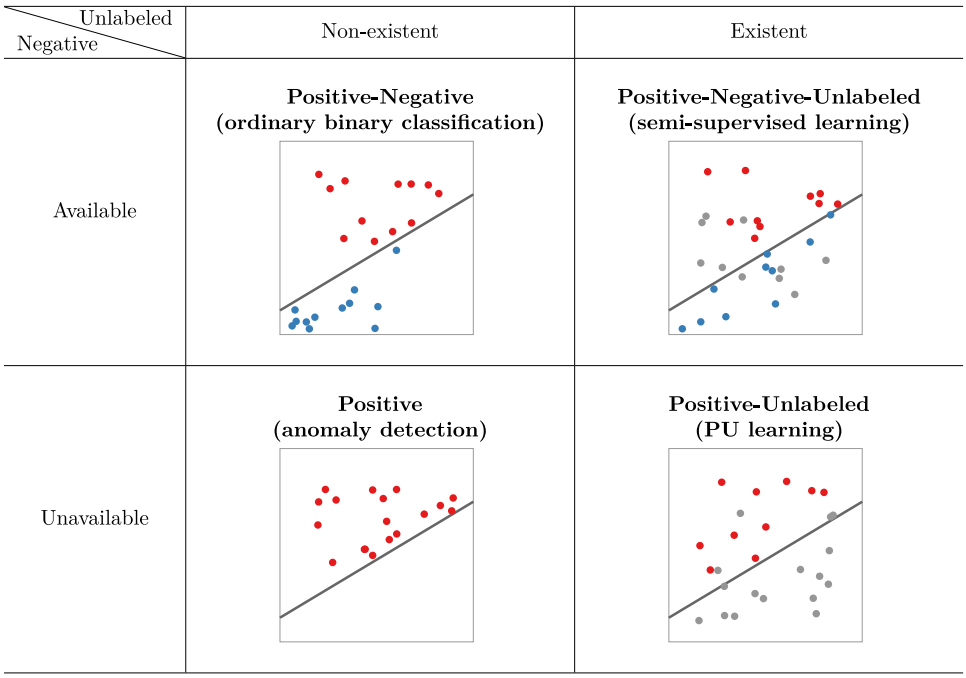

Fig. 2 Classification of problem settings based on the availability of negative label information and the existence of unlabeled data samples in training dataset. Positive, negative, and unlabeled data points are shown in red, blue, and gray, respectively

Here, we explain uPU (unbiased positive-unlabeled) learning (du Plessis et al. 2014) and nnPU (non-negative positive-unlabeled) learning (Kiryo et al. 2017), which are closely related to our approach. Let $X \in \mathbb{R}^d$ and $Y \in \{+1, -1\}$ denote the input and output random variables, respectively. Let $p(\boldsymbol{x}, y)$ denote the joint probability distribution over (X, Y), and let $p_{pos}(\boldsymbol{x}) = p(\boldsymbol{x}|Y = +1)$, $p_{neg}(\boldsymbol{x}) = p(\boldsymbol{x}|Y = -1)$, and $p_{unl}(\boldsymbol{x}) = p(\boldsymbol{x})$ denote the conditional probability density functions for the positive, negative, and unlabeled categories, respectively. We assume that the data distribution of the unlabeled data is expressed in terms of the conditional probabilities of positive and negative data, which implies that $p_{unl}(\boldsymbol{x}) = \pi_{pos} p_{pos}(\boldsymbol{x}) + \pi_{neg} p_{neg}(\boldsymbol{x})$ holds. In addition, let $g : \mathbb{R}^d \to \mathbb{R}$ denote a decision function, and let $l : \mathbb{R} \to \mathbb{R}$ denote a loss function, where $l(t, y)$ represents the loss value when the predicted value is t and the ground truth (correct label) is y. If the dataset consists of positive data $\{\boldsymbol{x}_1^{pos}, ..., \boldsymbol{x}_{m_{pos}}^{pos}\}$ and negative data $\{\boldsymbol{x}_1^{neg}, ..., \boldsymbol{x}_{m_{neg}}^{neg}\}$, the risk, which represents the expected loss value $\hat{R}_{pn}(g)$, is estimated as

$$\hat{R}_{pn}(g) = \pi_p \hat{R}_p^+(g) + \pi_n \hat{R}_n^-(g),$$

where $\hat{R}_p^+(g) = (1/m_{pos}) \sum_{k=1}^{m_{pos}} l(g(\boldsymbol{x}_k^{pos}), +1)$ and $\hat{R}_n^-(g) = (1/m_{neg}) \sum_{k=1}^{m_{neg}} l(g(\boldsymbol{x}_k^{neg}), -1)$. If positive data and unlabeled data $\{\boldsymbol{x}_1^{unl}, ..., \boldsymbol{x}_{m_{unl}}^{unl}\}$ are given, we use the relation $\pi_{neg} p_{neg}(\boldsymbol{x}) = p_{unl}(\boldsymbol{x}) - \pi_{pos} p_{pos}(\boldsymbol{x})$ to estimate risk $\hat{R}_{pu}(g)$:

$$\hat{R}_{pu}(g) = \pi_p \hat{R}_p^+(g) - \pi_p \hat{R}_p^-(g) + \hat{R}_u^-(g),$$

where $\hat{R}_p^-(g) = (1/m_{pos}) \sum_{k=1}^{m_{pos}} l(g(\boldsymbol{x}_k^{pos}), -1)$ and $\hat{R}_u^-(g) = (1/m_{unl}) \sum_{k=1}^{m_{unl}} l(g(\boldsymbol{x}_k^{unl}), -1)$, which corresponds to the methods used in uPU learning (du Plessis et al. 2014). In nnPU learning (Kiryo et al. 2017), the risk is adjusted to $\tilde{R}_{pu}(g)$, which is defined as

$$\tilde{R}_{pu}(g) = \pi_p \hat{R}_p^+(g) + \max\{0, \hat{R}_u^-(g) - \pi_p \hat{R}_p^-(g)\},$$

to ensure a non-negative risk value because uPU learning sometimes leads to overfitting when applied to models such as deep neural networks. Since the coefficient of $\hat{R}_u^-$ in the above equation is positive, nnPU learning can be considered effective for quantum state data, for which unlabeled data is likely to be predicted as negative, and negative data is expected to be abundant.

Semi-supervised learning (Ruff et al. 2020; Hsieh et al. 2019) is another problem setting for utilizing unlabeled data. Unlike PU learning, it includes a small amount of negative data.

3 Training entanglement detector using positive-unlabeled learning framework

For the problem setting described in section 2.1, we devised a method that integrates entanglement detection with nnPU learning (Kiryo et al. 2017) to train an entanglement detector

using only a realistically available dataset. In this section, we describe the proposed method and explain the process of data generation.

3.1 Proposed method

First, we briefly describe the proposed method. This method is designed for learning and inference in a classical system and is based on the assumption that exact values can be obtained for the density matrix used as input. This assumption facilitates model implementation based on the nnPU learning method (Kiryo et al. 2017). An overview of the proposed method is shown in Fig. 3.

The proposed method is primarily divided into two phases: data generation and model application. In the data generation phase, data corresponding to the density matrix is generated as positive data in separable states and as unlabeled data in states that are valid quantum states (refer to Theorem 1) although it is unknown whether these states are separable or entangled. Here, we examine the process of data generation using quantum circuits with random operations under depolarizing noise, starting from an initial state, such as state $|\psi_{init}\rangle = |0\rangle^{\otimes n}$. When constructing a dataset for entanglement detection, it is desirable that the dataset be capable of spanning all possible states that may exist as either separable or entangled from the perspective of data quality. In this problem setting, labeling entangled states is generally more difficult than labeling separable states due to the following factors.

Difficulty of labeling based solely on input information In classical machine learning applications, annotation work is often performed to assign labels to unlabeled data. For example, when determining whether characters or specific features are present in an input image, human experts can often assess the accuracy of an image simply by looking at it. However, in entanglement detection, it is common to use density matrices or estimates of expected values of certain physical quantities as input. In such cases, it is often impossible for humans to determine entanglement solely on the basis of these numerical data.

Non-guaranteed separable/entangled states after global random operations When generating data to span the possible separable states, these states can be spanned by performing local unitary operations within each qubit. However, when generating data to span the possible entangled states, global random operations across qubits are required. These operations do not necessarily guarantee that the resulting states are entangled (see Fig. 4).

In considering ways to avoid the difficulty of assigning labels to negative data, it is logical to develop learning methods, such as PU learning, that do not depend on negative labels so that they can be applied to more practical problem settings.

In the model application phase, the generated density matrix data are used as input, and the final output is a real scalar value indicating the degree of separability or entanglement. In an n-qubit system, the density matrix is represented as a complex matrix of size $2^n \times 2^n$. In the proposed method, this matrix decomposed into its real and imaginary components and input as a real tensor of size $2^n \times 2^n \times 2$. The reasons for adopting this input format are as follows.

Input format of density matrices The proposed method is designed to take a density matrix input. However, vectors

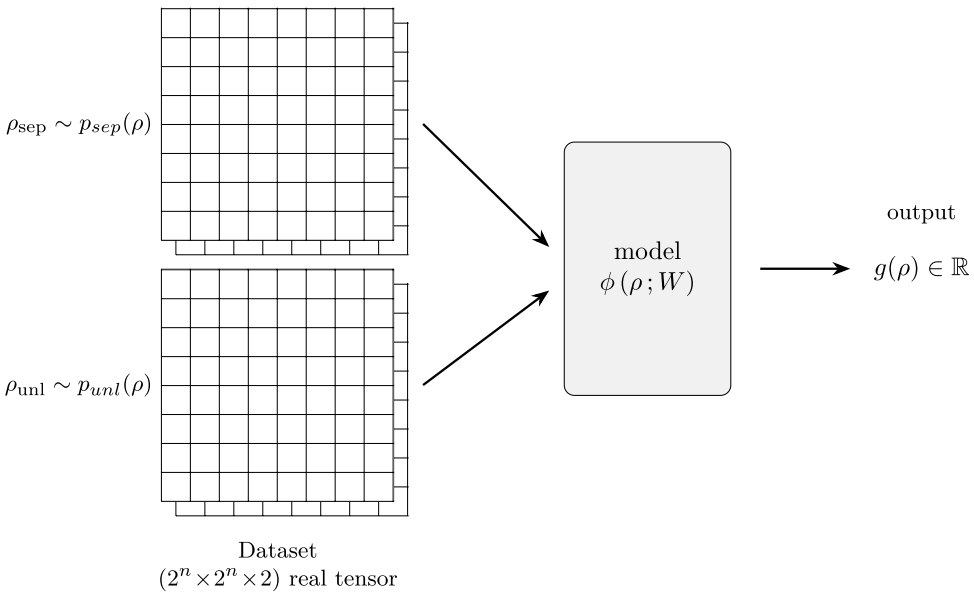

Fig. 3 Overview of proposed method

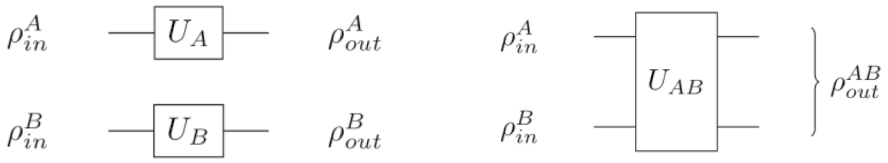

(a) process to generate separable states (b) process to generate entangled states

Fig. 4 Processes for generating separable and entangled states. Although preparing entangled data is challenging due to verification difficulties, the output state is reliably classified as unlabeled

consisting of the expected values of physical quantities, such as Pauli observables, can also be used to represent quantum states. We chose the density matrix format for input due to its compatibility with classical shadow methods (Huang et al. 2020). These methods store snapshots of the density matrix of a quantum state, enabling estimation of the original density matrix values from their expectation values. The number of snapshots can be adjusted in accordance with the required accuracy, enabling the generation of density matrices with arbitrary accuracy. Given this flexibility, we adopted the density matrix format in this study.

Input format: Real tensor representation of density matrices While density matrices are inherently complex, our method represents them as real-valued tensors by decomposing them into their real and imaginary parts. This approach offers several advantages. 1) Ease of combination with machine learning frameworks: In machine learning research, real number input problem settings are more common than complex number input ones, and model implementation is mainly based on the assumption that the inputs are given as real values. Additionally, models that take color images as input often use input formats, such as $32 \times 32 \times 3$ and $224 \times 224 \times 3$, that are similar to the $2^n \times 2^n \times 2$ format of real-valued density matrices. This suggests that image input models may be readily adapted for density matrix input models. 2) Adaptability and performance considerations: Although some studies suggest that methods tailored for complex inputs might offer performance improvements (Trabelsi et al. 2018), such benefits are highly dependent on the specific problem setting and dataset. We used the real number input format in the proposed method, considering both the convenience of using real number inputs and the performance variations when using complex number inputs.

This method produces real scalar values that are used to calculate the AUC—a metric commonly used PU learning and anomaly detection. When binary classification is desired (i.e., assigning labels $\{+1, -1\}$), applying an appropriate threshold to these real values enables evaluation using the AUC or F1 score.

3.2 Data generation

When framing the entanglement detection problem as a machine learning problem, one key challenge is that the distribution ranges of positive and negative example data are adjacent. This closeness can lead to misclassification even with slight shifts in the classification boundary, creating a substantial obstacle to reliable classification. For robust evaluation of models trained on such problems, it is crucial that the dataset contains a substantial number of samples near the true classification boundary. Standard entangled states—such as GHZ states, W states, and their locally transformed variants— typically do not span the region near the classification boundary. Relying solely on such states may therefore adversely affect model evaluation. To address this limitation, we generate a synthetic dataset based on a Hilbert-Schmidt measure-based data distribution combined with the PPT criterion (Theorem 2). This approach ensures that a large amount of the generated data is near the classification boundary between separable and entangled states, thereby enabling a more comprehensive assessment of model performance.

Data distribution of density matrix in Hilbert-Schmidt measure Here we describe the data distribution used in our experiments. Density matrices for an *n*-qubit state were sampled using the following procedures (Zyczkowski and Sommers 2001) with $N = 2^n$.

1. Let A, B be $N \times N$ matrices in which each element A_{jk} and $B_{jk} (1 \leq j, k \leq N)$ is independently drawn from the standard normal distribution, i.e., $\mathcal{N}(0, 1)$.
2. Construct an $N \times N$ complex matrix C with entries defined as $C_{jk} = A_{jk} + iB_{jk}$.
3. Define density matrix ρ as $\rho = CC^\dagger / \mathrm{Tr}[CC^\dagger]$, which ensures that ρ meets the conditions for a valid density matrix (see Theorem 1).

For two qubits, it has been suggested that the probability of a density matrix generated by this method being separable is 8/33, or approximately 24% (Slater 2007).

Creation of dense synthetic datasets using PPT criterion To create the dense datasets described above, we used the

PPT criterion. This method enables perfect classification when the exact values of the density matrix elements are clearly identified, as in specific systems such as two-qubit systems. In the context of determining fully-separability, we use the PPT criterion to construct a dataset including entangled state data near classification boundary. Chen et al. (2021) reported an implementation for two-qubit systems based on a similar approach, and we believe that it can be extended to systems with three or more qubits. Specifically, we would generate density matrices ρ for an n-qubit system as follows: For predetermined indices $a, b (1 \leq a < b \leq n)$,

$$\rho_{j_1 \ldots j_n, k_1 \ldots k_n} = \rho^1_{j_1,k_1} \cdots \rho^{a-1}_{j_{a-1},k_{a-1}} \rho^{a+1}_{j_{a+1},k_{a+1}} \cdots \rho^{b-1}_{j_{b-1},k_{b-1}} \rho^{b+1}_{j_{b+1},k_{b+1}} \cdots \rho^{n}_{j_n,k_n} \rho^{ab}_{j_a j_b, k_a k_b}.$$

where $j_1, \ldots, j_n, k_1, \ldots, k_n \in \{1, 2\}$ and $\rho_{j_1 \ldots j_n, k_1 \ldots k_n}$ represents the element located at the $(\sum_{l=1}^{n} (j_l - 1) * 2^{n-l} + 1)$ -th row and $(\sum_{l=1}^{n} (k_l - 1) * 2^{n-l} + 1)$-th column in ρ. This indexing convention is similarly applied to the following matrices: ρ^{ab}, which a 4×4 density matrix according to Hilbert-Schmidt measure described above, and 2×2 density matrices, which are sampled similarly. When $b = a + 1$, the overall density matrix can be expressed more simply as

$$\rho = \rho^1 \otimes \cdots \otimes \rho^{a-1} \otimes \rho^{ab} \otimes \rho^{b+1} \otimes \cdots \otimes \rho^n$$

A dataset generated using this formulation is adjacent to the fully-separable data on the entangled side, ensuring coverages near the target classification boundary.

4 Related work

Various methods have been explored for using machine learning to detect entanglement. This section summarizes the most relevant research. Table 1 provides an overview of related work. The abbreviations used in the table are as follows: FCNN (fully-connected neural network), AE (autoencoder), LSTM (long short-term memory), CNN (convolutional neural network), SNN (Siamese neural network), SVM (support vector machine), AutoML (automated machine learning), QNN (quantum neural network), QSVM (quantum support vector machine), and RBM (restricted boltzmann machine).

Neural network-based approaches are among the most prevalent methods for entanglement detection using machine learning. Roik et al. (2021) investigated the effect of the number of measurements on classification performance, while Ureña et al. (2024) examined how deep models respond to variations in data distribution. Chen et al. (2022) presented methods for classifying GME using a neural network, and Singh et al. (2025) introduced an approach

Table 1 A part of the studies and its comparison on entanglement detection using machine learning methods

References	Methods	Data availability		
		P	N	U
Roik et al. (2021)	FCNN	✓	✓	
Ureña et al. (2024)	″	✓	✓	
Singh et al. (2025)	″	✓	✓	
Asif et al. (2023)	″	✓	✓	
Ma and Yung (2018)	″	✓	✓	
Gao et al. (2024)	″	✓	✓	
Li et al. (2025)	″	✓	✓	
Qu et al. (2023)	FCNN,AE	✓	✓	
Huang et al. (2025)	FCNN,LSTM	✓	✓	
Luo et al. (2024)	CNN	✓	✓	
Li et al. (2024)	CNN,Transformer	✓	✓	
Pawłowski and Krawczyk (2024)	CNN,SNN	✓	✓	
Sanavio et al. (2023)	SVM	✓	✓	
Vintskevich et al. (2023)	″	✓	✓	
Greenwood et al. (2023)	″	✓	✓	
Rosebush et al. (2024)	″	✓	✓	
Lu et al. (2018)	Bagging	✓	✓	
Goes et al. (2021)	AutoML	✓	✓	
Yin et al. (2022)	QNN	✓	✓	
Scala et al. (2022)	″	✓	✓	
Sharma et al. (2025b)	QSVM	✓	✓	
Harney et al. (2020)	RBM			✓
Harney et al. (2021)	″			✓
Krawczyk et al. (2024)	AE			✓
Chen et al. (2021)	CNN,SNN	✓		
Zhang et al. (2023)	FCNN	✓	✓	✓
Luo et al. (2023)	SVM	✓	✓	✓
Ours	CNN	✓		✓

based on deep neural networks with feature selection. Additionally, Asif et al. (2023) presented a method using features based on relative entropy, while Ma and Yung (2018) introduced a method using features derived from Bell's inequality within neural networks. Further, Lu et al. (2018) explored methods based on convex hull approximation in connection with ensemble learning, and this technique has also been employed in Wang (2022), which utilizes SLOCC (stochastic local operations and classical communication) for data generation. Casalé et al. (2023) also proposed a method based on convex hull approximation for systems other than qubits. Chen et al. (2020) demonstrated the use of neural networks to assess the entanglement structure of the noisy quantum generalized GHZ state. Gulati et al. (2024) concentrated on the standard form of input features and developed a technique for reducing dimensionality. Tian et al. (2022) developed an optimization method for

models that accounts for the effects of experimental noise. Trávníček et al. (2024) proposed a detection method that utilizes supervised learning through estimation of negativity. Rizvi et al. (2022) proposed a classification approach predicated on the characteristics of observables in relation to entanglement states. Khalid et al. (2024) focused on detecting fundamental quantum resources, which are more general than entanglement detection, and proposed a detection method using fully connected neural networks. Huang et al. (2025) presented a method of detecting entanglement using only information from local measurements.

Several studies have explored entanglement detection methods designed specifically for matrix-based input representations. Luo et al. (2024) introduced a convolutional neural network model for GME verification and demonstrated its effectiveness in environments with specified noise. Khoo and Heyl (2021) proposed a classification method based on statistical images derived from the transverse-field ferromagnetic Ising model. Li et al. (2024) presented a hybrid approach combining a convolutional neural network and a Transformer model to distinguish between W states and GHZ states. They later proposed a multi-view neural network model with the objective of reducing computational cost (Li et al. 2025). XpookyNet, as introduced in Kookani et al. (2024), focuses on reducing the number of measurements required during training. Qu et al. (2023) developed a complex-valued autoencoder model applicable to qubit systems of up to four qubits. Additionally, Pawłowski and Krawczyk (2024) presented a model that accounts for invariances in entanglement properties under to local unitary operations and qubit permutations. Soubusta et al. (2025) advanced a computational resource-aware classification method for entanglement.

In addition to neural network-based methods, several studies have explored alternative machine learning techniques for entanglement detection. Sanavio et al. (2023) proposed constructing entanglement witness operators using a support vector machine to classify unknown input quantum states. Other SVM-based approaches have been reported (Vintskevich et al. 2023; Xu and Zhao 2022). Greenwood et al. (2023) introduced a methods that calculates the expectations of selected Pauli observables—quantities that are computationally efficient to evaluate—and uses them as features for entanglement detection tasks. In relation to this method, Rosebush et al. (2024) enhanced efficiency in terms of computational complexity. Martínez-Sabiote et al. (2025) proposed a method employing support vector machine for entanglement detection in high-dimensional systems. These approaches use a two-class SVM to solve classical binary classification problems. Additionally, Harney et al. (2020) presented a method using restricted Boltzmann machines for entanglement detection in pure states. Subsequently, they expanded the methodology to encompass the application in mixed states (Harney et al. 2021). Shokou and Yeganeh (2025) proposed a hybrid approach combining quantum neural networks with classical fully connected neural networks. Sekuła et al. (2025) investigated the efficacy of Transformer models when presented with millions of training data points for the purposes of pre-training and fine-tuning. Krawczyk et al. (2024) proposed a methodology employing autoencoders to ascertain the separability of quantum states. Sá and Roditi (2021) presented an empirical discussion of the challenges associated with training entanglement classifiers based solely on information from local measurements. Yosefpor et al. (2020) proposed a method leveraging neural networks to ascertain optimal measurements in the entanglement detection problem. Fuchs et al. (2025) demonstrated the generation and detection of entanglement on quantum hardware using manifold learning. Goes et al. (2021) reported on the effectiveness of AutoML in the detection of entanglement. Zia et al. (2025) proposed utilizing quantum extreme learning machines for entanglement witnessing. Ahmed et al. (2021) conducted exhaustive experiments and discussions on a range of topics, including the classification of quantum states in optical systems. Sun et al. (2024) verified the performance of detection in scenarios where measurements are incomplete. Khalid et al. (2025) proposed the concept of a universal quantum witness machine, which would be utilized for the study of fundamental properties of quantum systems.

For formulation as one-class classification, Chen et al. (2021) introduced a deep learning approach based on ideas from Siamese networks and GANs. Their method frames entanglement detection as an anomaly detection problem, a type of unsupervised learning. To achieve this they developed methods that rely exclusively on separable data.

The concept of utilizing quantum states as unlabeled data has been explored in various research studies. Zhang et al. (2023) devised a semi-supervised learning method and used it to demonstrate how using unlabeled data can enhance entanglement detection. Luo et al. (2023) enhanced the performance of semi-supervised SVMs for GME state classification using techniques such as grouping unlabeled data and using iterative labeling.

Related research has expanded in various directions, Brunner et al. (2024) characterized the separability of states using methods based on manifold learning embedding techniques. Yin et al. (2022) formulated the entanglement detection problem as a two-player zero-sum game, and solved it using a quantum neural network. Gao et al. (2024) applied a neural network to a continuous-variable problem setting. Scala et al. (2022) investigated parametrized quantum circuits as a model for constructing entanglement witness

operators. K et al. (2024) formulated entanglement detection as a multi-armed bandit problem and proposed a detection algorithm with probabilistic theoretical guarantees. Sharma et al. (2025b) have proposed a cross-domain classification method that utilizes quantum support vector machines. They later proposed a classification method employing quantum neural networks in conjunction with a problem-inspired data generation circuit (Sharma et al. 2025a). Mahdian and Mousavi (2025) investigated the feasibility of entanglement detection in a real quantum computer environment. Qiu et al. (2019) investigated the use of discrete-variable quantum neural networks and continuous-variable quantum neural networks for the entanglement detection problem.

5 Numerical experiments

We conducted numerical experiments to evaluate the effectiveness of the proposed PU learning-based framework for entanglement detection. To assess whether incorporating unlabeled data as training data enhances classifier performance, we compared the performances of two baseline methods that use only positive data with that of the proposed method, which uses both positive data and unlabeled data. In ablation studies, we verified the behavior of the proposed method when changing the network and input features.

5.1 Methodology

Baseline methods We evaluated the proposed method using two one-class classification methods. Their hyperparameter settings were primarily based on their original implementations unless otherwise specified. One baseline method was the network introduced in Chen et al. (2021), which combines a Siamese network with a complex neural network. We refer to it as PS-CxGAN on the basis of its elements—a pseudo-Siamese network, a complex neural network, and a GAN. We used RMSProp optimizer with a momentum value 0.9, and set the learning rate to 10^{-4} for all 100 training epochs. A weight decay for PS-CxGAN was not applied. The other baseline method was the DeepSVDD model introduced in Ruff et al. (2018), in which DeepSVDD model is pretrained using autoencoder followed by training with a convolutional neural network. We used the Adam optimizer with a weight decay of 5×10^{-7} for pretraining and training, while keeping the default parameter settings for the other hyperparameters. The initial learning rate was set to 10^{-4} and reduced to 10^{-5} after 250 pretraining epochs and 100 training epochs. The DeepSVDD model was pretrained for 350 epochs and trained for 150 epochs.

Proposed method We used nnPU learning (Kiryo et al. 2017) as the PU learning method for entanglement detection. We used the Adam optimizer with a weight decay of 5×10^{-4} while the other hyperparameters were kept at their default values. The learning rate was set to 10^{-4} for all 100 training epochs, a value lower than that used in the original implementation. For all three methods, the batch size was fixed at 128.

5.2 Architectures

To minimize performance differences arising from variations in model parameters and structure, we aligned the architecture of the three methods with those of PS-CxGAN and DeepSVDD for each comparison. The resulting architectures are shown in Table 2.

Here we denote a convolutional layer with kernel size k and d output channels as $C[d \times (k \times k)]$, while a linear layer is specified solely by its number of output units. For the PS-CxGAN-based method, we applied batch normalization between convolutional layers and used the ReLU activation function between layers, including linear layers. In this method, half of the channel and unit numbers are used to represent the real and imaginary parts, respectively. Therefore, the total number of channels and units remains constant. For the DeepSVDD-based method, we applied batch normalization, followed by the leaky ReLU activation function, and a 2×2 max pooling operation, in that order between convolutional layers. We omitted both the batch normalization parameters and the bias term in the linear layer of the DeepSVDD method to prevent hypersphere collapse (Ruff et al. 2018).

Table 2 Network architecture used in numerical experiments. The same network architecture was used for each method except for the number of units in the final layer(*). Only the nnPU method changed the final output dimension to 1

	PS-CxGAN-based network
2-qubit	$C[20 \times (2 \times 2)] - C[60 \times (2 \times 2)] - 240 - 192 - 20^*$
3-qubit	$C[20 \times (3 \times 3)] - C[60 \times (3 \times 3)] - C[60 \times (3 \times 3)] - 240 - 192 - 20^*$
	DeepSVDD-based network
4-qubit	$C[32 \times (5 \times 5)] - C[64 \times (5 \times 5)] - 1024 - 64^*$
5-qubit	$C[32 \times (5 \times 5)] - C[64 \times (5 \times 5)] - C[128 \times (5 \times 5)] - 2048 - 128^*$
6-qubit	$C[32 \times (5 \times 5)] - C[64 \times (5 \times 5)] - C[128 \times (5 \times 5)] - C[256 \times (5 \times 5)] - 4096 - 256^*$

5.3 Setup

Our synthesized dataset include PU data representing density matrices of fully-separable states and entangled states—meaning the dataset contained two labels. We used only positive label data for the one-class classification methods and both positive and unlabeled data for the proposed method. The dataset consisted of 60,000 training samples and 12,000 test samples, both of which included the same number of positive and negative samples, i.e., $\pi_p = 0.5$. The synthesized dataset contained 20,400 explicit positive samples and 39,600 unlabeled samples, with all 30,000 negative samples included in the unlabeled data. This means that the ratio of positive samples within the unlabeled data was 8/33, based on sampling from the Hilbert-Schmidt measure. To ensure equality in the amount of data between the compared methods, we conducted additional experiments using a subdataset of 6,000 positive-unlabeled samples (1/10 samples) for the proposed method. These samples were selected to maintain the same ratio of labeled data as in the original set of 60,000 samples (full samples).

5.4 Results

The experimental results are shown in Table 3, where each value represents the average and standard deviation from five trials using different seeds. As shown in Table 3, the proposed PU learning-based method achieved better performance than the baseline methods. Although the results of nnPU using 1/10 samples were lower than those using full samples, it's reasonable, but they showed high performance compared to the baseline methods. In this problem setting, it was assumed that the positive data spanned most of the true positive data set, leading to the expectation that the baseline methods would perform similarly to the proposed method. However, the results contradict this expectation. One possible explanation is as follows. According to Bekker and Davis (2020), in one-class classification, the negative class (e.g., entangled state) is not included in the given sample (positive class, e.g., separable state) and is instead considered as all other possible classes. Conversely, in the context of PU learning, unlabeled samples offer insights into the global distribution of data, encompassing the potential presence of negative samples. From this standpoint, access to valid density matrix data may have been a contributing factor to the high performance of the PU learning method in this study. Additionally, we remark that data points from the positive class and negative class are close to each other in the feature space. Consequently, in one-class classification methods, that exclusively utilize positive samples, even if the given positive data can be classified as belonging to the positive class (data closer to the positive boundary), it is expected to be challenging to correctly classify negative data as negative. In PS-CxGAN, for instance, the classification of data outside the region of positive data as negative requires the generation of data within the negative data region and the training of the discriminator to accurately differentiate between the two. However, in this problem setting, there is no explicit incentive, such as a loss function design, to generate negative data uniformly across all regions where negative data could potentially exist. In scenarios where positive and negative data are distributed near the classification boundary, ambiguity in learning the boundary may contribute to suboptimal performance. Conversely, the PU learning approach involves the provision of information regarding unlabeled samples. Moreover, given that the information regarding negative samples is provided through a class prior, in conjunction with the positive data information, it is conceivable to predict points that are likely to be negative.

5.5 Ablation studies

To analyze the impact of the components of the proposed method, we conducted ablation studies in a setting with 1/10 samples of 5-qubit quantum states. We examined the effects of introducing complex neural networks (Trabelsi et al. 2018) and input features. 1) Application of complex neural networks: complex neural networks handle input and network parameters within the range of complex numbers. These networks perform operations based on complex numbers and are also used in the PS-CxGAN baseline method (Chen et al. 2021). In this ablation study, we replaced the convolution layer, the activation function and batch normalization with a complex neural network. We conducted experiments using the $\mathbb{C}$ReLU activation function (Trabelsi et al. 2018). 2)

Table 3 Experimental results. The values below show the averages and standard deviations of the execution results for five different seeds. The nnPU results show the case of using 6,000 samples (1/10 samples) and 60,000 samples (full samples) as training data

	PS-CxGAN	DeepSVDD	nnPU(1/10 samples)	nnPU(full samples)
2-qubit	0.9889 ± 0.0217	0.9713 ± 0.0067	0.9967 ± 0.0005	0.9998 ± 0.0001
3-qubit	0.5153 ± 0.0617	0.6521 ± 0.0324	0.9579 ± 0.0103	0.9972 ± 0.0003
4-qubit	0.4738 ± 0.0216	0.5371 ± 0.0072	0.9150 ± 0.0070	0.9928 ± 0.0012
5-qubit	0.4619 ± 0.0277	0.4179 ± 0.0147	0.8783 ± 0.0125	0.9862 ± 0.0050
6-qubit	0.4884 ± 0.0127	0.3925 ± 0.0096	0.8359 ± 0.0116	0.9846 ± 0.0031

Input features: In addition to density matrices, quantum states can be represented as sets of expected values of observed quantities. One such representation is the expected values of Pauli observables, which can concisely represent quantum states. Here, we evaluate the performance of using Pauli observables as features, where they are represented as 4^5-dimensional vectors. We used a fully connected neural network with the output sizes of $200-200-200-1$ as the network architecture. For comparison, we conducted additional experiments using feature vectors consisting of 4^5 values. These values were obtained by extracting the diagonal components and the real and imaginary parts of the non-diagonal components from the density matrix. The experimental results are shown in Table 4.

The experimental results for complex neural networks, were lower than those obtained using conventional neural networks. This result suggests that treating it is appropriate to treat the inputs as real numbers in this problem setting.

One factor contributing to the poorer performance of complex neural networks compared to real neural networks is the issue of inductive bias in complex neural networks. Specifically, the limited parameter freedom in the convolution operations within complex neural networks did not align well with the problem setting at hand. In complex neural networks, given a complex filter matrix $W = A + iB\,(A, B \in \mathbb{R}^{k\times k})$ of kernel size k and the $m \times m$ complex matrix $H = X + iY\,(X, Y \in \mathbb{R}^{m\times m})$, the convolution operation between each channel pair within complex neural networks is expressed as

$$W * H = (A + iB) * (X + iY) = (A * X - B * Y) + i(B * X + A * Y)$$

where * denotes the convolution operation between two real matrices. Note that in the above convolution operation, the contribution to the real part of X and the contribution to the imaginary part of Y are performed through the same single real matrix A (the same applies to B). That is, the ratio of contribution to the real and imaginary parts of the input values is fixed. Conversely, the density matrix, which is the input feature in this problem setting, has real diagonal entries by definitions so the distribution of real and imaginary values differs for each matrix element. Considering this, convolving the real part X and imaginary part Y with values of the same scale may excessively restrict the model's representation. Meanwhile, in real neural networks, the filter matrix parameters are independent between each channel pair. This suggests that the model's expressive power is higher, leading to superior performance compared to complex neural networks. Here we remark that Trabelsi et al. (2018) states that the difference in classification performance between real and complex models regarding experimental results on complex neural networks varies depending on the dataset, task, and architecture. We believe it is important to note that our results do not necessarily imply outcomes for different problem settings.

For the results for the input features, a significant difference was observed in the one-sided t-test at the significance level 0.05. This result was a bit surprising because the two types of features can be mapped one-to-one by an affine transformation. That is, considering that the features $\boldsymbol{x}_d$ obtained from the density matrix and the features $\boldsymbol{x}_p$ obtained from the Pauli observables, there are the weights W_d, W_p and the biases $\boldsymbol{b}_d, \boldsymbol{b}_p$ of the first-layer linear layer satisfy the relation $\boldsymbol{z} = W_d\boldsymbol{x}_d + \boldsymbol{b}_d = W_p\boldsymbol{x}_p + \boldsymbol{b}_p$. These results seem to suggest that the performance of entanglement detection may be sensitively affected by feature selection. To strengthen our confidence in this point, we conducted an additional ablation study.

Further investigation and experimentation on this point led us to conclude that there is no significant difference in the information held by at least the Pauli observables and density matrices regarding label inference, and that the key point lies in the scale of the features. To analyze the impact of feature selection on model performance, we first calculated N2 and N3 for our test dataset of 5-qubit, complexity metrics for binary classification problem proposed by Ho and Basu (2002). These metrics estimate the difficulty of learning based solely on the input features, with N2 and N3 specifically calculated from the information of nearest neighbor samples in the feature space. Specifically, N2 is the average ratio of intra-class to inter-class distances for each data point. N3, on the other hand, is the proportion of data points for which the nearest neighbor belongs to a different class. In other words, large values of N2 and N3 indicate that training the dataset is difficult. The specific calculation results are shown in Table 5.

As a result, highly similar values were obtained. These results suggest that feature selection does not significantly affect classification based on nearest neighbors. Further investigation into the difference in the distribution of input feature values confirmed that the standard deviation of features based on Pauli operators is tens of times larger than that of features based on the density matrix. In this study, which utilizes quantum states distributed in or near

Table 4 Experimental results in ablation studies. The values below show the averages and standard deviations of the execution results for five different seeds

1) Complex NNs		2) Input features	
Complex NNs	Real NNs	Pauli observables	Density matrices
0.8246 ± 0.0190	0.8783 ± 0.0125	0.6309 ± 0.0040	0.6521 ± 0.0096

Table 5 Metrics for estimating the difficulty of training datasets

	Pauli observables	Density matrices
N2	0.4944	0.4945
N3	0.4368	0.4329

fully separable regions, the values of each element in the density matrix decrease exponentially with the number of qubits. Conversely, the absolute values of the Pauli operator often become larger. This is thought to cause the difference in standard deviation. In machine learning models incorporating weight decay, increasing the absolute magnitude of features can excessively boost the model's expressive power, as features with larger absolute values contribute more significantly to the output when weights are fixed. To verify this, we conducted experiments examining performance changes when features were fixed and weight decay was increased. The results are shown in Table 6.

Increasing weight decay from the initial setting raised the AUC score, and in the one-sided t-test at the significance level 0.05, no significant difference was observed compared to using the density matrices features. We consider these additional observations to support the notion that there is no significant difference between Pauli observables and density matrices regarding feature design. At the same time, we also believe they suggest that attention should be paid to the scale and distribution of values when designing features, even in situations where the domain is fixed to the range of $[-1, +1]$ due to the use of density matrices and Pauli observables.

6 Discussion

We proposed using a PU learning-based learning method to address the problem of generating data for entanglement detection. Here, we clearly state the limitations of our method. One of the major limitations of the proposed method is that it is not scalable for larger systems. In short, applying the proposed method directly to larger systems is likely to face scalability issues. Consider a simple example: the behavior of the proposed method when increasing the number of qubits while keeping the number of steps and the number of samples in the dataset constant. First, the size of a single density matrix increases exponentially, meaning the dataset size would also increase exponentially. Furthermore, the size of the neural network model used–specifically, the number of parameters within the model–also increases exponentially relative to the qubit count when scaled using a design like the DeepSVDD-based network described in the paper. Overall, computational complexity, training time, and memory usage are expected to scale exponentially with the number of qubits. We discuss the approach to the scaling problem in conclusion.

7 Conclusion

Through this paper, we have demonstrated that learning methods based on positive-unlabeled learning are well suited to the entanglement detection problem, particularly given the constraints of realistically obtainable datasets. Numerous studies have highlighted the potential of machine learning approaches for entanglement detection, establishing them as promising candidates for creating general-purpose entanglement detectors. However, as noted in Chen et al. (2021), it is essential to consider the practical challenges of data acquisition when implementing these approaches. From this perspective, we propose treating states with no guarantee of separability or entanglement as unlabeled data and incorporating them into a PU learning framework. PU learning is a well-established field in machine learning that provides insights applicable to other fields. In particular, the nnPU learning method (Kiryo et al. 2017) used in our experiments is designed to avoid overfitting when applying deep models, making it an effective approach for the application of these models in classical systems. Moreover, our comparative experiments demonstrated the superiority of the proposed method. Methods based on PU learning effectively utilize information in unlabeled data and tend to maintain high performance in entanglement detection even when data is concentrated near the classification boundary.

As future work, we may explore the following problems:

Scaling problem Scaling is a fundamental challenge in quantum computing, and the entanglement detection approach presented in this paper is no exception. One straightforward solution to scaling is to perform most of the learning and inference directly in the quantum domain. In this case, constructing a high-quality dataset becomes a crucial issue to be addressed. Although dataset generation was touched upon in our description of the proposed method, ensuring a comprehensive representation of entangled states through quantum operations remains a difficult task, as

Table 6 Additional experimental results in ablation studies. The values below show the averages and standard deviations of the execution results for five different seeds

Input		Pauli observables		Density matrices
Weight decay	5×10^{-4}	5×10^{-3}	5×10^{-2}	5×10^{-4}
AUC	0.6309 ± 0.0040	0.6475 ± 0.0089	0.6592 ± 0.0063	0.6521 ± 0.0096

spanning the entire space of entangled states is inherently complex. Although research on dataset construction has been conducted (Schatzki et al. 2021; Perrier et al. 2022), preparing datasets for large systems remains a key challenge for future studies. As an alternative approach, exploring memory-efficient classical methods could be beneficial. Feature selection (Singh et al. 2025), a well-established technique in classical machine learning, may also be applicable to entanglement detection. If an efficient feature selection method can be identified, it could enable the application of classical frameworks to relatively large systems.

Variations in problem setting Since there are various types of entanglement, it is important to investigate its detailed properties using variational formulations in entanglement detection. Examples include formulations as regression problems and with generalized classification boundaries. In formulating the task as a regression problem, we can consider predicting such as predicting values such as a certain type of entropy. Various studies have quantified entropy values using deep learning (Koutný et al. 2023; Gray et al. 2018), so applying the PU learning framework to this field is conceivable. Generalizing the classification boundary involves, for example, determining whether a given state is k-separable (Gabriel et al. 2010), which includes fully-separable classification problem. The ability to classify using more diverse boundaries may make the methods described in this paper applicable to a wider range of situations.

Acknowledgements This work was partially supported by JST SPRING Grant Number JPMJSP2119 and JSPS KAKENHI Grant Number JP22K19820.

Author Contributions T. Nohara designed the study, wrote the main manuscript, and conducted all of the experiments under the supervision of I. Noda and S. Oyama.

Data Availability Dataset used during the current study are available from the corresponding author on reasonable request.

Declarations

Competing interests The authors declare no competing interests.

References

Ahmed S, Sánchez Muñoz C, Nori F et al (2021) Classification and reconstruction of optical quantum states with deep neural networks. Phys Rev Res 3:033278. https://doi.org/10.1103/PhysRevResearch.3.033278

Asif N, Khalid U, Khan A et al (2023) Entanglement detection with artificial neural networks. Sci Rep 13:1562. https://doi.org/10.1038/s41598-023-28745-3

Bekker J, Davis J (2020) Learning from positive and unlabeled data: a survey. Mach Learn 109:719–760. https://doi.org/10.1007/s10994-020-05877-5

Bennett CH, Brassard G (2014) Quantum cryptography: Public key distribution and coin tossing. Theoret Comput Sci 560:7–11. https://doi.org/10.1016/j.tcs.2014.05.025

Brunner E, Xie A, Dufour G, et al (2024) Data-driven approach to mixed-state multipartite entanglement characterisation. Preprint at https://arxiv.org/abs/2407.18014

Casalé B, Molfetta GD, Anthoine S, et al (2023) Large-scale quantum separability through a reproducible machine learning lens. Preprint at https://arxiv.org/abs/2306.09444

Chen C, Ren C, Lin H, et al (2020) Entanglement structure detection via machine learning. Preprint at https://arxiv.org/abs/2012.00526

Chen Y, Pan Y, Zhang G et al (2021) Detecting quantum entanglement with unsupervised learning. Quantum Science and Technology 7(1):015005. https://doi.org/10.1088/2058-9565/ac310f

Chen Z, Lin X, Wei Z (2022) Certifying unknown genuine multipartite entanglement by neural networks. Preprint at https://arxiv.org/abs/2210.13837

Dür W, Vidal G, Cirac JI (2000) Three qubits can be entangled in two inequivalent ways. Phys Rev A 62:062314. https://doi.org/10.1103/PhysRevA.62.062314

du Plessis MC, Niu G, Sugiyama M (2014) Analysis of learning from positive and unlabeled data. In: Ghahramani Z, Welling M, Cortes C et al (eds) Advances in Neural Information Processing Systems, vol 27. Curran Associates Inc

Elkan C, Noto K (2008) Learning classifiers from only positive and unlabeled data. In: Proceedings of the 14th ACM SIGKDD International Conference on Knowledge Discovery and Data Mining. Association for Computing Machinery, New York, NY, USA, KDD '08, p 213–220, https://doi.org/10.1145/1401890.1401920

Fuchs AJC, Brunner E, Seong J et al (2025) Machine-learning certification of multipartite entanglement for noisy quantum hardware. New J Phys 27(7):074501. https://doi.org/10.1088/1367-2630/adde80

Gabriel A, Hiesmayr BC, Huber M (2010) Criterion for k-separability in mixed multipartite systems. Preprint at https://arxiv.org/abs/1002.2953

Gao X, Isoard M, Sun F et al (2024) Correlation-pattern-based continuous variable entanglement detection through neural networks. Phys Rev Lett 132:220202. https://doi.org/10.1103/PhysRevLett.132.220202

Gühne O, Tóth G (2009) Entanglement detection. Phys Rep 474(1):1–75. https://doi.org/10.1016/j.physrep.2009.02.004

Goes CBD, Canabarro A, Duzzioni EI, et al (2021) Automated machine learning can classify bound entangled states with tomograms. Quantum Information Processing 20(3). https://doi.org/10.1007/s11128-021-03037-9

Gray J, Banchi L, Bayat A et al (2018) Machine-learning-assisted many-body entanglement measurement. Phys Rev Lett 121:150503. https://doi.org/10.1103/PhysRevLett.121.150503

Greenwood AC, Wu LT, Zhu EY et al (2023) Machine-learning-derived entanglement witnesses Phys Rev Appl 19:034058. https://doi.org/10.1103/PhysRevApplied.19.034058

Grover LK (1996) A fast quantum mechanical algorithm for database search. In: Proceedings of the Twenty-Eighth Annual ACM Symposium on Theory of Computing, Philadelphia, Pennsylvania, USA, pp 212–219, https://doi.org/10.1145/237814.237866

Gulati V, Siyanwal S, Arvind, et al (2024) Ann-enhanced detection of multipartite entanglement in a three-qubit nmr quantum processor. Preprint at https://arxiv.org/abs/2409.19739

Gurvits L (2003) Classical deterministic complexity of edmonds' problem and quantum entanglement. In: Proceedings of the Thirty-Fifth Annual ACM Symposium on Theory of Computing. Association for Computing Machinery, New York, NY, USA, STOC '03, p 10–19, https://doi.org/10.1145/780542.780545, the long version is available at https://arxiv.org/abs/quant-ph/0303055

Harney C, Pirandola S, Ferraro A et al (2020) Entanglement classification via neural network quantum states. New J Phys 22(4):045001. https://doi.org/10.1088/1367-2630/ab783d

Harney C, Paternostro M, Pirandola S (2021) Mixed state entanglement classification using artificial neural networks. New J Phys 23(6):063033. https://doi.org/10.1088/1367-2630/ac0388

Ho TK, Basu M (2002) Complexity measures of supervised classification problems. IEEE Trans Pattern Anal Mach Intell 24(3):289–300. https://doi.org/10.1109/34.990132

Horodecki M, Horodecki P, Horodecki R (1996) Separability of mixed states: necessary and sufficient conditions. Phys Lett A 223(1):1–8. https://doi.org/10.1016/S0375-9601(96)00706-2

Horodecki M, Horodecki P, Horodecki R (1999) General teleportation channel, singlet fraction, and quasidistillation. Phys Rev A 60:1888–1898. https://doi.org/10.1103/PhysRevA.60.1888

Hsieh YG, Niu G, Sugiyama M (2019) Classification from positive, unlabeled and biased negative data. In: Proceedings of the 36th International Conference on Machine Learning, Proceedings of Machine Learning Research, vol 97. PMLR, pp 2820–2829

Huang HY, Kueng R, Preskill J (2020) Predicting many properties of a quantum system from very few measurements. Nat Phys 16:1050–1057. https://doi.org/10.1038/s41567-020-0932-7

Huang Y, Che L, Wei C, et al (2025) Direct entanglement detection of quantum systems using machine learning. npj Quantum Information 11(1):29. https://doi.org/10.1038/s41534-025-00970-w

Ju H, Lee D, Hwang J et al (2020) Pumad: Pu metric learning for anomaly detection. Inf Sci 523:167–183. https://doi.org/10.1016/j.ins.2020.03.021

K B, Siddhu V, Jagannathan K (2024) Classical bandit algorithms for entanglement detection in parameterized qubit states. Preprint at https://arxiv.org/abs/2406.19738

Khalid U, Duong TQ, Shin H (2024) Artificial neural networks for quantum sensing: Metrologically resourceful state detection. In: 2024 International Conference on Quantum Communications, Networking, and Computing (QCNC), pp 259–264, https://doi.org/10.1109/QCNC62729.2024.00048

Khalid U, Ur Rehman J, Jung H et al (2025) Quantum property learning for nisq networks: Universal quantum witness machines. IEEE Trans Commun 73(4):2207–2221. https://doi.org/10.1109/TCOMM.2024.3469555

Khoo JY, Heyl M (2021) Quantum entanglement recognition Phys Rev Res 3:033135. https://doi.org/10.1103/PhysRevResearch.3.033135

Kiryo R, Niu G, du Plessis MC, et al (2017) Positive-unlabeled learning with non-negative risk estimator. In: Advances in Neural Information Processing Systems, vol 30. Curran Associates, Inc

Kookani A, Mafi Y, Kazemikhah P, et al (2024) Xpookynet: Advancement in quantum system analysis through convolutional neural networks for detection of entanglement. Preprint at https://arxiv.org/abs/2309.03890

Koutný D, Ginés L, Moczała-Dusanowska M, et al (2023) Deep learning of quantum entanglement from incomplete measurements. Science Advances 9(29):eadd7131. https://doi.org/10.1126/sciadv.add7131

Krawczyk M, Pawłowski J, Maśka MM et al (2024) Data-driven criteria for quantum correlations. Phys Rev A 109:022405. https://doi.org/10.1103/PhysRevA.109.022405

Li R, Du J, Qin Z et al (2024) Entanglement structure detection via computer vision. Phys Rev A 110:012448. https://doi.org/10.1103/PhysRevA.110.012448

Li R, Zhang S, Qin Z et al (2025) Low-cost detection of high-dimensional multipartite entanglement structures. Phys Rev Appl 23:044033. https://doi.org/10.1103/PhysRevApplied.23.044033

Lu S, Huang S, Li K et al (2018) Separability-entanglement classifier via machine learning. Phys Rev A 98:012315. https://doi.org/10.1103/PhysRevA.98.012315

Luo YJ, Liu JM, Zhang C (2023) Detecting genuine multipartite entanglement via machine learning. Phys Rev A 108:052424. https://doi.org/10.1103/PhysRevA.108.052424

Luo YJ, Leng X, Zhang C (2024) Genuine multipartite entanglement verification with convolutional neural networks. Phys Rev A 110:042412. https://doi.org/10.1103/PhysRevA.110.042412

Ma YC, Yung MH (2018) Transforming bell's inequalities into state classifiers with machine learning. npj Quantum Information 4(1):34. https://doi.org/10.1038/s41534-018-0081-3

Mahdian M, Mousavi Z (2025) Entanglement detection with quantum support vector machine (qsvm) on near-term quantum devices. Sci Rep 15(1):11931. https://doi.org/10.1038/s41598-025-95897-9

Martínez-Sabiote A, Skotiniotis M, Bermejo-Vega JJ, et al (2025) Entanglement detection with quantum-inspired kernels and svms. Preprint at https://arxiv.org/abs/2508.17909

Nielsen MA, Chuang IL (2010) Quantum Computation and Quantum Information: 10th, Anniversary. Cambridge University Press

Pawłowski J, Krawczyk M (2024) Identification of quantum entanglement with siamese convolutional neural networks and semisupervised learning. Phys Rev Appl 22:014068. https://doi.org/10.1103/PhysRevApplied.22.014068

Peres A (1996) Separability criterion for density matrices. Phys Rev Lett 77:1413–1415. https://doi.org/10.1103/PhysRevLett.77.1413

Perrier E, Youssry A, Ferrie C (2022) Qdataset, quantum datasets for machine learning. Scientific Data 9(1):582. https://doi.org/10.1038/s41597-022-01639-1

Qiu PH, Chen XG, Shi YW (2019) Detecting entanglement with deep quantum neural networks. IEEE Access 7:94310–94320. https://doi.org/10.1109/ACCESS.2019.2929084

Qu YD, Zhang RQ, Shen SQ et al (2023) Entanglement detection with complex-valued neural networks. Int J Theor Phys 62(9):206. https://doi.org/10.1007/s10773-023-05460-3

Rizvi SMA, Asif N, Ulum MS, et al (2022) Multiclass classification of metrologically resourceful tripartite quantum states with deep neural networks. Sensors 22(18). https://doi.org/10.3390/s22186767

Roik J, Bartkiewicz K, Černoch A et al (2021) Accuracy of entanglement detection via artificial neural networks and human-designed entanglement witnesses. Phys Rev Appl 15:054006. https://doi.org/10.1103/PhysRevApplied.15.054006

Rosebush AR, Greenwood ACB, Kirby BT et al (2024) An exponential reduction in training data sizes for machine learning derived entanglement witnesses. Machine Learning Science and Technology 5(3):035068. https://doi.org/10.1088/2632-2153/ad7457

Ruff L, Vandermeulen R, Goernitz N, et al (2018) Deep one-class classification. In: Dy J, Krause A (eds) Proceedings of the 35th International Conference on Machine Learning, Proceedings of Machine Learning Research, vol 80. PMLR, pp 4393–4402

Ruff L, Vandermeulen RA, Görnitz N, et al (2020) Deep semi-supervised anomaly detection. In: 8th International Conference on

Learning Representations, ICLR 2020, Addis Ababa, Ethiopia, April 26-30, 2020

Sá N, Roditi I (2021) β-variational autoencoder as an entanglement classifier. Phys Lett A 417:127697. https://doi.org/10.1016/j.physleta.2021.127697

Sanavio C, Tignone E, Ercolessi E (2023) Entanglement classification via witness operators generated by support vector machine. The European Physical Journal Plus 138:936. https://doi.org/10.1140/epjp/s13360-023-04546-5

Scala F, Mangini S, Macchiavello C, et al (2022) Quantum variational learning for entanglement witnessing. In: 2022 International Joint Conference on Neural Networks (IJCNN), pp 1–8, https://doi.org/10.1109/IJCNN55064.2022.9892080

Schatzki L, Arrasmith A, Coles PJ, et al (2021) Entangled datasets for quantum machine learning. Preprint at https://arxiv.org/abs/2109.03400

Sekuła P, Romaszewski M, Głomb P, et al (2025) Quantum-aware transformer model for state classification. Preprint at https://arxiv.org/abs/2502.21055

Seliya N, Zadeh AA, Khoshgoftaar TM (2021) A literature review on one-class classification and its potential applications in big data. Journal of Big Data 8:122. https://doi.org/10.1186/s40537-021-00514-x

Sharma D, Sabale VB, M. T, et al (2025a) Quantum neural networks facilitating quantum state classification. Preprint at https://arxiv.org/abs/2504.06622

Sharma D, Sabale VB, Singh P et al (2025) Harnessing quantum support vector machines for cross-domain classification of quantum states. Quantum Machine Intelligence 7(1):49. https://doi.org/10.1007/s42484-025-00274-4

Shokou MR, Yeganeh HD (2025) Hybrid quantum-classical learning of nonlinear entanglement witnesses via continuous-variable quantum neural networks. Preprint at https://arxiv.org/abs/2509.05924

Shor P (1994) Algorithms for quantum computation: discrete logarithms and factoring. In: Proceedings 35th Annual Symposium on Foundations of Computer Science, pp 124–134

Singh J, Gulati V, Dorai K et al (2025) Entanglement classification of arbitrary three-qubit states via artificial neural networks. Phys Rev Appl 24:034069. https://doi.org/10.1103/xfks-snj1

Slater PB (2007) Dyson indices and hilbert–schmidt separability functions and probabilities. J Phys A: Math Theor 40(47):14279–14308. https://doi.org/10.1088/1751-8113/40/47/017

Soubusta J, Černoch A, Lemr K (2025) Deep-learned classification of quantum correlations from collective measurements. Phys Lett A 559:130911. https://doi.org/10.1016/j.physleta.2025.130911

Sun Q, Song Y, Liao Z, et al (2024) High-accuracy entanglement detection via a convolutional neural network with noise resistance. Applied Sciences 14(20). https://doi.org/10.3390/app14209418

Takahashi H, Iwata T, Kumagai A, et al (2024) Deep positive-unlabeled anomaly detection for contaminated unlabeled data. Preprint at https://arxiv.org/abs/2405.18929

Tax DM, Duin RP (2004) Support vector data description. Mach Learn 54:45–66. https://doi.org/10.1023/B:MACH.0000008084.60811.49

Thew RT, Nemoto K, White AG et al (2002) Qudit quantum-state tomography. Phys Rev A 66:012303. https://doi.org/10.1103/PhysRevA.66.012303

Tian Y, Che L, Long X et al (2022) Machine learning experimental multipartite entanglement structure. Advanced Quantum Technologies 5(10):2200025. https://doi.org/10.1002/qute.202200025

Trabelsi C, Bilaniuk O, Zhang Y, et al (2018) Deep complex networks. In: 6th International Conference on Learning Representations, ICLR 2018

Ureña J, Sojo A, Bermejo-Vega J et al (2024) Entanglement detection with classical deep neural networks. Sci Rep 14:18109. https://doi.org/10.1038/s41598-024-68213-0

Trávníček V, Roik J, Bartkiewicz K et al (2024) Sensitivity versus selectivity in entanglement detection via collective witnesses. Phys Rev Res 6:033056. https://doi.org/10.1103/PhysRevResearch.6.033056

Vidal G, Werner RF (2002) Computable measure of entanglement. Phys Rev A 65:032314. https://doi.org/10.1103/PhysRevA.65.032314

Vintskevich SV, Bao N, Nomerotski A et al (2023) Classification of four-qubit entangled states via machine learning. Phys Rev A 107:032421. https://doi.org/10.1103/PhysRevA.107.032421

Wang P (2022) A convex hull-based machine learning algorithm for multipartite entanglement classification. Applied Sciences 12(24). https://doi.org/10.3390/app122412778

Xu J, Zhao Q (2022) Towards efficient and generic entanglement detection by machine learning. Preprint at https://arxiv.org/abs/2211.05592

Yin XF, Du Y, Fei YY et al (2022) Efficient bipartite entanglement detection scheme with a quantum adversarial solver. Phys Rev Lett 128:110501. https://doi.org/10.1103/PhysRevLett.128.110501

Yosefpor M, Mostaan MR, Raeisi S (2020) Finding semi-optimal measurements for entanglement detection using autoencoder neural networks. Quantum Science and Technology 5(4):045006. https://doi.org/10.1088/2058-9565/aba34c

Zhang L, Chen Z, Fei SM (2023) Entanglement verification with deep semisupervised machine learning. Phys Rev A 108:022427. https://doi.org/10.1103/PhysRevA.108.022427

Zhao Y, Xu Q, Jiang Y, et al (2022) Dist-pu: Positive-unlabeled learning from a label distribution perspective. In: Proceedings of the IEEE/CVF Conference on Computer Vision and Pattern Recognition (CVPR), pp 14461–14470

Zhou Y, Zhao Q, Yuan X, et al (2019) Detecting multipartite entanglement structure with minimal resources. npj Quantum Information 5(1):83. https://doi.org/10.1038/s41534-019-0200-9

Zia D, Innocenti L, Minati G, et al (2025) Quantum extreme learning machines for photonic entanglement witnessing. Preprint at https://arxiv.org/abs/2502.18361

Zyczkowski K, Sommers HJ (2001) Induced measures in the space of mixed quantum states. J Phys A: Math Gen 34(35):7111–7125. https://doi.org/10.1088/0305-4470/34/35/335